

1 **THYROID MALT LYMPHOMA: SELF-HARM TO GAIN POTENTIAL T-CELL HELP**

2 Fangtian Wu,^{1,2} Natsuko Watanabe,³ Maria-Myrsini Tzioni,¹ Ayse Akarca,⁴ Chunye Zhang,¹ Yan Li,^{1,5} Zi
3 Chen,¹ Francesco Cucco,¹ Natasha Carmell,⁶ Jaeduk Yoshimura Noh,³ Koichi Ito,⁷ Rachel Dobson,¹
4 Sarah Moody,¹ Wenqing Yao,^{1,8} Wenyan Zhang,⁸ Weiping Liu,⁸ Hongxiang Liu,⁹ Jessica Okosun,¹⁰
5 Andreas Chott,¹¹ Yingwen Bi,¹² Shih-Sung Chuang,¹³ Markus Raderer,¹⁴ Jian-Yong Li,² Teresa
6 Marafioti,⁴ Ming-Qing Du^{1,15}

7

8 ¹Division of Cellular and Molecular Pathology, Department of Pathology, University of Cambridge,
9 Cambridge, UK;

10 ²Department of Hematology, Pukou CLL Center, the First Affiliated Hospital of Nanjing Medical
11 University, Jiangsu Province Hospital, Collaborative Innovation Center for Cancer Personalized
12 Medicine, Nanjing 210029, PR China;

13 ³Department of Internal Medicine, Ito Hospital, Tokyo 150-8308, Japan;

14 ⁴Department of Pathology, University College London, London, UK.

15 ⁵Department of Haematology, Hebei General Hospital, Shijiazhuang, Hebei, PR China;

16 ⁶Indica Labs, Albuquerque, NM 87114, United States;

17 ⁷Department of Surgery, Ito Hospital, Tokyo 150-8308, Japan;

18 ⁸Department of Pathology, West China Hospital, Sichuan University, Chengdu, PR China;

19 ⁹Molecular Malignancy Laboratory, Addenbrooke's Hospital, Cambridge University Hospitals NHS
20 Foundation Trust, Cambridge, UK;

21 ¹⁰Centre for Haemato-Oncology, Barts Cancer Institute, Queen Mary University of London, London,
22 UK;

23 ¹¹Institute of Pathology and Microbiology, Wilhelminenspital, Vienna, Austria;

24 ¹²Department of Pathology, Eye & ENT Hospital, Fudan University, Shanghai, PR China;

25 ¹³Department of Pathology, Chi-Mei Medical Centre, Tainan, Taiwan;

26 ¹⁴Department of Medicine I, Clinical Division of Oncology, Medical University of Vienna, Austria;

27 ¹⁵Department of Histopathology, Addenbrooke's Hospital, Cambridge University Hospitals NHS
28 Foundation Trust, Cambridge, UK;
29

30 **Running title:** *CD274* and *TNFRSF14* mutation in thyroid lymphoma

31 **Key words:** *CD274*, *TNFRSF14*, *TET2*, mutation, thyroid MALT lymphoma, autoimmunity

32 **Word Count:** Abstract: 200; the main manuscript text: 3779

33 **Manuscript figure and tables:** 7 Figures, 6 Supplementary Figures, 6 Supplementary Tables

34

35 Correspondence to

36 Professor Ming-Qing Du,

37 Division of Cellular and Molecular Pathology,

38 Department of Pathology, University of Cambridge

39 Box 231, Level 3, Lab Block, Addenbrooke's Hospital,

40 Hills Road, Cambridge, CB2 2QQ, United Kingdom

41 Tel: +44 (0)1223 767092; Fax: +44 (0)1223 586670; Email: mqd20@cam.ac.uk

42

43 **Sources of Research support:** The research in MQD's lab was supported by grants from Bloodwise
44 (13 006, 15 019) UK, the Kay Kendall Leukaemia Fund (KKL582) UK. FW was supported by a research
45 fellowship from the China Scholarship Council, and a research award from the Addenbrooke's
46 Charitable Trust. WY was supported by a research fellowship from the China Scholarship Council,
47 and an International Collaborative Award from the Pathological Society of Great Britain and Ireland,
48 UK. The Human Research Tissue Bank is supported by the NIHR Cambridge Biomedical Research
49 Centre.

50

51 **ABSTRACT**

52 The development of extranodal marginal zone lymphoma of mucosa-associated lymphoid tissue
53 (MALT) is driven by chronic inflammatory responses and acquired genetic changes. To investigate its
54 genetic bases, we performed targeted sequencing of 93 genes in 131 MALT lymphomas including 76
55 from the thyroid. We found frequent deleterious mutations of *TET2* (86%), *CD274* (53%), *TNFRSF14*
56 (53%) and *TNFAIP3* (30%) in thyroid MALT lymphoma. *CD274* was also frequently deleted, together
57 with mutation seen in 68% of cases. There was a significant association between *CD274*
58 mutation/deletion and *TNFRSF14* mutation ($P=0.001$). *CD274* (PD-L1) and *TNFRSF14* are ligands for
59 the co-inhibitory receptor PD1 and BTLA on T-helper cells, respectively, their inactivation may free T-
60 cell activities, promoting their help to malignant B-cells. In support of this, both the proportion of
61 activated T-cells (CD4+CD69+/CD4+) within the proximity of malignant B-cells, and the level of
62 transformed blasts were significantly higher in cases with *CD274/TNFRSF14* genetic abnormalities
63 than those without these changes. Both *CD274* and *TNFRSF14* genetic changes were significantly
64 associated with Hashimoto's thyroiditis ($P=0.01$, $P=0.04$ respectively), and *CD274* mutation/deletion
65 additionally associated with increased erythrocyte sedimentation rate ($P=0.0001$). In conclusion,
66 *CD274/TNFRSF14* inactivation in thyroid MALT lymphoma B-cells may deregulate their interaction
67 with T-cells, promoting co-stimulations and impairing peripheral tolerance.

68

69 INTRODUCTION

70 Extranodal marginal zone lymphoma of mucosa-associated lymphoid tissue (MALT) commonly arises
71 in a background of a chronic inflammatory disorder at diverse sites. The chronic inflammation may
72 be caused by infection such as *Helicobacter pylori* (*H. pylori*) or autoimmunity, for example, Sjögren's
73 syndrome and Hashimoto's thyroiditis. The chronic inflammatory process triggers the development
74 of acquired MALT, which generates the "local" adaptive immune response i.e. T-cell dependent B-
75 cell maturation [1]. These adaptive immune responses are critical for the clonal selection of
76 marginal zone B-cells and their malignant transformation. Both B-cell receptor (BCR) signalling and
77 T-cell help play an important role in the evolution of MALT lymphoma cells.

78 There are several strands of evidence indicating that BCR signalling is operational in MALT lymphoma.
79 Histologically, the lymphoma cells always express surface immunoglobulin M (IgM), frequently show
80 blast transformation, plasma cell differentiation and follicular colonisation [2]. Their proliferation
81 can be stimulated by crosslinking their surface IgM [3]. Moreover, inhibiting BCR signalling with a
82 BTK inhibitor induces durable responses in patients with MALT lymphoma [4]. There is mounting
83 evidence to suggest that MALT lymphoma associated BCRs are autoreactive, albeit largely based on
84 findings from those of the salivary gland, ocular adnexa and stomach [1]. In ocular adnexal MALT
85 lymphoma, there is a significant association between the biased usage of autoreactive IGHV4-34 and
86 inactivation of *TNFAIP3* (A20) [5], which encodes a global negative regulator of the canonical NF- κ B
87 pathway. The findings suggest oncogenic cooperation between chronic BCR signalling and its
88 downstream genetic change, thus advocating their cooperative role in clonal selection and
89 malignant transformation.

90 The understanding of the role of T-cell help in MALT lymphoma pathogenesis is largely based on
91 observations from the gastric form. Early studies show that gastric MALT lymphoma B-cells respond
92 to *H. pylori* stimulation *in vitro*, but this critically depends on tumour infiltrating T-cells involving

93 CD40/CD40L co-stimulating molecules [6-8]. Subsequent animal model studies confirm the above
94 observations, and also demonstrate that T-helper cells are indispensable for tumour growth *in vivo*
95 [9,10]. Since T-cell dependent B-cell maturation is the cardinal feature of the adaptive immune
96 responses, T-cell help may represent a common mechanism in the pathogenesis of MALT
97 lymphomas regardless of their sites. T-cell help may also cooperate with BCR signalling and somatic
98 genetic changes in the clonal evolution of lymphoma cells.

99 To unravel the genetic basis and improve our understanding on the oncogenic cooperation between
100 genetic changes and tumour environment, we recently performed whole exome sequencing (WES)
101 analyses of 21 MALT lymphomas of the salivary glands and thyroid [11]. This identified recurrent
102 novel mutations in several genes encoding G-protein coupled receptor (GPCR), including *GPR34* and
103 *CCR6*, and lead to the discovery of a significant association between *GPR34* and *TBL1XR1* mutations
104 in salivary gland MALT lymphoma [11]. *GPR34* mutations are activating changes, promoting the
105 receptor signalling, while the *TBL1XR1* mutations appear to enhance the transcriptional activities of
106 NF- κ B and AP1 by mediating nuclear receptor corepressor degradation [12]. Again, *GPR34* and
107 *TBL1XR1* mutations are potentially cooperative events, providing another example linking surface
108 receptor signalling to downstream genetic changes. To extend this discovery, we have designed a
109 panel of 93 genes including GPCR genes implicated in lymphocyte biology, the genes mutated in
110 marginal zone lymphoma and also those showing isolated but potentially pathogenic mutation from
111 our previous WES study, such as *CD274* [11]. By targeted sequencing of this gene panel in MALT
112 lymphoma of various sites, we have identified highly frequent inactivating mutations of both *CD274*
113 (PD-L1) and *TNFRSF14* in thyroid MALT lymphoma. PD-L1 and TNFRSF14 inactivation in malignant B-
114 cells may eliminate their inhibitory regulation to T-helper cells, indirectly enhancing their activities,
115 and hence exaggerating their help to tumour B-cells.

116

117 MATERIALS AND METHODS

Case selection and materials

Local ethical guidelines were followed for the use of archival tissues for research with ethical approval (05-Q1604-10). A total of 194 cases of lymphoma were successfully investigated, including 131 MALT lymphomas [thyroid n=76, ocular adnexa n=30, salivary gland (mainly *GPR34* mutation negative cases) n=17, others n=8], splenic marginal zone lymphoma (SMZL n=18), follicular lymphoma (n=20), angioimmunoblastic T-cell lymphoma (AITL, n=19) and monomorphic epitheliotropic intestinal T-cell lymphoma (n=6) (Table S1). Formalin-fixed paraffin-embedded (FFPE) diagnostic tissue biopsies or DNA samples were available in each case. Most of the thyroid MALT lymphomas were from Ito Hospital, Tokyo, with detailed clinical and laboratory data [13], and their diagnosis was ascertained by appropriate immunohistochemical and genetic analyses, particularly to exclude follicular lymphoma.

DNA extraction and quality assessment

For each specimen, tumour rich areas (>30%) were microdissected on FFPE slides. DNA was extracted using the QIAamp DNA Micro Kit (QIAGEN, UK) and quantified using a Qubit® Fluorometer (Life Technologies, UK). The quality of DNA samples was assessed by PCR of variably sized genomic fragments [14].

Gene panel for targeted sequencing

We comprehensively reviewed WES data on marginal zone lymphoma together with those from our previous study [11,15]. We also reviewed the GPCR literature and identified those involved in lymphocyte biology as we recently found recurrent GPCR mutations in MALT lymphoma [11]. Based on these reviews, we established a panel of 93 genes for MALT lymphoma, comprising those mutated in marginal zone lymphoma, the GPCR genes implicated in lymphocyte biology and those showing isolated but potentially pathogenic changes from our previous WES study, such as *CD274* (Table S2) [11].

HaloPlexHS enrichment and Illumina HiSeq sequencing

This was essentially performed as described previously using HaloPlexHS system and Illumina HiSeq4000 sequencing [14]. Experimental methods, variant calling and annotation, and validation of the newly designed gene panel are detailed in the supplementary materials (Figure S1 &S2).

Where indicated, the variants identified by targeted sequencing were confirmed by PCR and Sanger sequencing, and their somatic origin ascertained by analysis of DNA samples from microdissected non-neoplastic cells (Table S3, Figure S3).

Multiplex ligation-dependent probe amplification (MLPA)

CD274 deletion was investigated using the MLPA assay (MRC-Holland). The MLPA assay includes multiple probes for the *CD274* (7 probes), *PDCD1LG2* (10 probes) and *JAK2* (12 probes) locus together with controls, which are located within a 0.59 Mb region at 9p24.1. DNA from FFPE tonsil tissues were utilised as a normal diploid control for normalisation. Prior to data collection, various qualities and quantities of DNA samples were tested to establish the minimal sample requirements (>30% tumour cell content, 100ng input, strong amplification of ≥ 300 bp genomic fragment) for the assay. Data normalisation and analysis were performed using the Coffalyser.NET analysis software (MRC-Holland). The target/reference probe ratios were visualised using R-V3.6.1 and R studio.

Interphase fluorescence in situ hybridisation (FISH)

In thyroid MALT lymphoma, interphase FISH was performed to investigate *MALT1*, *FOXP1* and *IGH* translocations using break-apart probes [16].

Multiplex immunofluorescent staining (mIF)

FFPE tissue sections of thyroid MALT lymphomas and reactive tonsils were subjected to mIF staining using antibodies against Ki67/CD8, PD1, CD4, PD-L1, CD69 and CD20 sequentially (Table S4).

The antigen retrieval and mIF were performed on a Leica BOND RX automated immunostainer (Leica Microsystems, UK) using Opal 7-Color Automation IHC Kit (Akoya Biosciences, USA). Experimental conditions, validation, imaging acquisition and data analysis optimisation are detailed in the supplementary methods).

For data collection, tumour areas with adequate staining were identified, and representative diffuse tumour areas excluding colonised follicles were marked based on haematoxylin and eosin slide and mIF staining pattern. The expression of CD20, CD4, PD1 and CD69 and their co-expression in the selected diffuse tumour areas were quantified, and their spatial relationship was further analysed using the Halo-V3.1 Proximity Module accordingly.

PD-L1 immunohistochemistry

This was performed on FFPE tissue sections using an automated immunostainer (Bond-III system, Leica Biosystems). Following antigen retrieval by combination of heat and Bond Epitope Retrieval 2 solution for 20 minutes, PD-L1 was stained with the monoclonal antibody clone E1L3N (Cell Signalling) and visualized using Bond Polymer Kit.

Semi-quantification of histopathological features

The extent of transformed blasts, plasmacytic differentiation and follicular colonisation were semi-quantified using a three tiers system by two pathologists blindly. Any discrepancies were reviewed and rescored. The score criteria were as follows: transformed blasts: score 1 = 0-5 large cells per high power field (HPF), score 2 = 6-15 large cells per HPF, score 3 = >15 large cells per HPF; plasmacytic differentiation: score 0 = no plasmacytic differentiation, score 1 = focal or scattered plasmacytic differentiation, score 3 = diffuse areas of plasmacytic differentiation; and follicular colonisation: score 1 = no apparent follicular colonisation, score 1 = follicular colonisation in $\leq 50\%$ follicles, score 2 = follicular colonisation in $> 50\%$ follicles.

Statistical analysis

Comparison of *TET2*, *CD274*, *TNFRSF14* and *TNFAIP3* mutation AAF (alternative allele frequency) values were analysed using a paired t-test. Association among categorical variables were analysed using Chi-square test. Comparison of the duration of Hashimoto's thyroiditis between different mutation groups were performed using t-test. Comparison of semi-quantitative or quantitative phenotypical data were analysed using Wilcoxon rank sum test.

RESULTS

Frequent *CD274* and *TNFRSF14* mutations in thyroid MALT lymphoma

Among MALT lymphoma of various sites, the most prominent findings were frequent *CD274* (52.6%), *TNFRSF14* (52.6%), *TET2* (85.5%) and *TNFAIP3* (30%) mutations in the thyroid cases (Figure 1, Figure S4). The former three gene mutations were not or rarely seen in MALT lymphoma of other sites. The somatic nature of *CD274* and *TNFRSF14* mutations were confirmed in 15 and 17 cases respectively, for which sufficient non-neoplastic cells could be microdissected for sequencing analysis (Figure 2, Figure S3).

Most *CD274* mutations in thyroid MALT lymphoma were likely deleterious (Figure 2, Table S5). Of the 42 mutations detected in 40 cases, 23 were nonsense (11), frameshift indels (7) or changes involving the essential splicing site (5). These mutations were widely distributed, but always occurred upstream of the C-terminal transmembrane domain, predicting truncated products that are unlikely to be expressed on cell surface. The remaining 19 mutations were missense changes affecting the translation start site (5), PD1 binding sites (4), the transmembrane domain (2), the IgV-like or IgC-like domain (6) and regions with unknown functional domain (2).

Similarly, most *TNFRSF14* mutations in thyroid MALT lymphoma were also likely deleterious (Figure 2, Table S5). Of the 42 mutations identified, 16 were nonsense (9), frameshift indels (6) or changes involved the essential splicing site (1). These mutations were dispersed, but always upstream of the

213 C-terminal transmembrane domain, predicting truncated products that are unable to be expressed
 214 on cell surface. The remaining 26 mutations were missense changes, which primarily affected the
 215 translation start site (10), or clustered at the TNFR Cys1 (8) or Cys 3 domain (6).

216 The *TET2* mutations seen in thyroid MALT lymphoma were very similar to those found in AITL
 217 (Figure 2, Table S5) [17]. Of the 65 cases with *TET2* mutations, 30 had two mutations. Of the 95
 218 mutations detected, 71 were nonsenses (29), frameshift indels (40) or changes affecting the
 219 essential splicing site (2). These mutations were widely distributed, predicting for variably truncated
 220 protein products. The remaining 24 mutations were missense changes (22) and inframe deletions
 221 (2), and largely clustered in the cysteine rich and double-stranded β helix domains, which were
 222 essential for the integrity of the overall structure and the catalytic activity of TET2 [18].

223 *TNFAIP3* was also frequently mutated in thyroid MALT lymphoma. A total of 31 *TNFAIP3* mutations
 224 were seen in 23 cases, and they comprised of nonsenses (8), frameshift indels (16) and changes
 225 affecting the essential splicing site (3) (Figure 2, Table S5). These mutations were widely dispersed,
 226 predicting variably truncated protein products. The remaining 4 mutations were missense changes
 227 (3) and inframe insertion (1) in the OTU domain.

228 Mutations in other genes at $\geq 3\%$ frequency identified in thyroid MALT lymphoma are shown in
 229 Figure 1, with full data presented in Figure S4. Among the 60 GPCR genes investigated, recurrent
 230 changes were seen in *CXCR5*, *CXCR3* and *CCR6* and characterised by clustered deleterious mutations
 231 in their C-terminal sequence but upstream of the phosphorylation site (Figure 2), which mediates
 232 interaction with β -arrestin and receptor internalization [19].

233 Interphase FISH showed a low frequency (7%) of *FOXP1*, but not *MALT1* translocation in thyroid
 234 MALT lymphoma (Figure 1). *IGH* translocation was seen in 26% of cases, including 4 of the 5 cases
 235 with *FOXP1* translocation.

236 **High *TET2* and *TNFRSF14* mutation AAF in thyroid MALT lymphoma**

237 *TET2* mutation occurs early in haematopoietic stem cells, typically in individuals with clonal
238 haematopoiesis of indeterminate potential. We correlated *TET2*, *TNFRSF14*, *CD274* and *TNFAIP3*
239 mutation AAF in thyroid MALT lymphoma in order to understand the sequence of their occurrence
240 (Figure 3). There was no difference in the AAF values between *TET2* and *CD274*, nor between *TET2*
241 and *TNFRSF14*, suggesting that the *TET2* mutations seen in thyroid lymphoma were most likely
242 lymphoma cell specific. Both *TET2* and *TNFRSF14* had a significantly higher AAF than *TNFAIP3*,
243 suggesting that *TNFAIP3* mutations may occur later than *TET2* and *TNFRSF14* changes.

244 As *TET2*, a methylcytosine dioxygenase, may influence DNA mutagenicity, and Tet deficient germinal
245 centre B-cells showed hypersomatic mutations skewing towards transition changes [20,21], we
246 compared mutation burden and spectrum according to the *TET2* mutation status in thyroid MALT
247 lymphoma (Figure 4). The number of somatic variants (excluding SNPs) was significantly higher in
248 the cases with *TET2* mutation than those without the mutation ($P=0.03$). The proportion of
249 transition mutations was also higher in cases with *TET2* mutation than those without the mutation,
250 although not reaching a statistical significance (Figure 4).

251 ***CD274* is also frequently targeted by deletion**

252 As *CD274* mutations were most likely inactivating changes, we further investigated whether *CD274*
253 was targeted by deletion. Of the 34 cases successfully investigated by MLPA, 21 showed deletion
254 involving the *CD274* locus. In 18 cases, the deletion spanned a region from *JAK2* exon-4 to *CD274*
255 exon 2 or 3, and appeared to be heterozygous. While in the remaining 3 cases, the deletion involved
256 *JAK2*, whole *CD274* and most of *PDCD1LG2* locus, and was homozygous. *CD274* deletion was much
257 higher in cases with wild type *CD274* than those with *CD274* mutation (80% vs 47%, $P=0.079$) (Figure
258 1 & S5). As expected, there was a mutual exclusion between *CD274* double mutations and
259 homozygous deletion (Figure 1). Taken together, 68% of thyroid MALT lymphomas had *CD274*
260 mutation or deletion or both. This frequency was likely underestimated as the deletion was not
261 investigated in a high proportion of cases with wild type *CD274* due to suboptimal DNA quality.

Interestingly, *CD274* mutation/deletion were significantly associated with *TNFRSF14* ($P=0.0013$), but not *TET2* mutation ($P=0.31$). There was no association between the *TNFRSF14* and *TET2* mutations.

Absence or low level of PD-L1 expression in thyroid MALT lymphoma

PD-L1 immunohistochemistry showed no detectable protein expression in the tumour cells of 51 thyroid MALT lymphomas investigated including 35 cases with *CD274* mutation/deletion (Figure S6). In each case, PD-L1 expression was seen in germinal centre macrophages, the thyroid epithelial cells involved in lymphoepithelial lesions but not in intact thyroid follicle.

Increased activated T-cells in the proximity of tumour B-cells in cases with *CD274/TNFRSF14* genetic changes

A total of 23 cases were successfully investigated by mIF including 17 cases with *CD274* mutation/deletion and/or *TNFRSF14* mutation, and 6 cases without these genetic changes (Figure 5). Overall, there were no significant differences in the ratio of CD4+ T-cells/CD20+ B-cells (Figure 5B), and the proportion of CD4+CD69+/CD4+, CD4+PD1+/CD4+, and CD4+CD69+PD1+/CD4+ T-cells between cases with and without *CD274/TNFRSF14* genetic changes.

As the effect of PD-L1 (*CD274*)/*TNFRSF14* inactivation to other cells is likely to be within the proximity of malignant B-cells, we quantified CD4+ T-cells and their immunophenotypic subsets (CD4+CD69+, CD4+PD1+, CD4+CD69+PD1+) within 10µm of CD20+ B-cells using Halo-V3.1 proximity module. Interestingly, the proportion of CD4+CD69+/CD4+ T-cells within 10µm proximity of B-cells was significantly higher in cases with *CD274/TNFRSF14* genetic abnormalities than those without these genetic changes (Figure 5). There was a similar trend for the proportion of CD4+PD1+ and CD4+CD69+PD1+ T-cell subsets, but not reaching a statistical significance (Figure 5B).

***CD274/TNFRSF14* genetic changes significantly associate with increased transformed blasts**

Several histological features of MALT lymphoma including blast transformation, plasmacytic differentiation and follicular colonisation are likely driven by antigenic stimulation, possibly involving T-cell help. Among these features, increased transformed blasts were significantly higher in cases with *CD274/TNFRSF14* genetic changes than those without these changes (Figure 6). There was also an association between increased transformed blasts and elevated serum thyroid stimulating hormone (TSH) and lactate dehydrogenase (LDH), and between follicular colonisation and increased serum soluble IL2R (Table S6).

Correlation among genetic and clinical parameters

CD274 mutation/deletion was significantly associated with advanced age, Hashimoto's thyroiditis, and increased erythrocyte sedimentation rate (Table S6). Similarly, *TNFRSF14* mutation was significantly associated with Hashimoto's thyroiditis. However, there was no association between *TET2* mutation and the clinical and laboratory parameters investigated.

DISCUSSION

The present study shows for the first time frequent *CD274* (PD-L1) inactivation by mutation and deletion in a human tumour i.e. thyroid MALT lymphoma. Remarkably, *CD274* mutations and deletions are significantly associated with a loss of function mutations of *TNFRSF14* in this low grade B-cell lymphoma, which typically arises from a background of autoimmune Hashimoto's thyroiditis. Given that PD-L1 and *TNFRSF14* are ligands for co-inhibitory receptors PD1 and BTLA on T-helper cells respectively, their inactivation may free T-cell activities and enhance their help to malignant B-cells. This speculation is supported by findings of higher proportions of activated T-cells in the vicinity of malignant B-cells, as well as increased levels of transformed blasts in cases with *CD274/TNFRSF14* genetic abnormalities.

CD274 (PD-L1) inactivation by mutation/deletion is highly restricted to thyroid MALT lymphoma, and rarely seen in MALT lymphoma of other sites or SMZL (Figure S4). In fact, these *PD-L1* genetic changes have not been reported in any human cancers despite the high volume of sequencing. On the contrary, *PD-L1* is targeted for over-expression by 9p24.1 amplification or chromosome translocation in a variety of solid tumours and lymphomas, particularly mediastinal large B-cell lymphoma and classic Hodgkin lymphoma [22-26]. This forms the molecular basis for immunotherapy with immune checkpoint inhibitors. These seemingly paradoxical observations strongly suggest a unique combination of aetiological, biological and oncogenic events during the multistage development of thyroid MALT lymphoma.

B and T-cells regulate each other's function during adaptive immune responses through concerted actions of their surface co-stimulatory [CD40/CD40L, CD80(CD86)/CD28] and co-inhibitory molecules (PD-L1/PD1, TNFRSF14/BTLA). Binding PD1 by PD-L1 attenuates T cell receptor (TCR) signalling and suppresses T-cell expansion and cytokine production. In mice with mixed bone marrow chimeras, PD-L1 deficient B-cells out-compete their wild-type counterpart in the germinal centre, memory and plasma cell compartments [27]. Conditional knockout of PD-L1 expression in B-cells does not affect B-cell development, but promotes earlier onset and increased inflammatory foci of experimental autoimmune encephalomyelitis in mice [28]. Similarly, binding BTLA by TNFRSF14 attenuates T-cell activation by reducing TCR signalling and CD40/CD40L interactions at the immunological synaptic interface, thus restraining its help to B-cells [29]. *Tnfrsf14* deficient B cells in mice show an enhanced growth advantage due to increased CD40/CD40L co-stimulation, and *Tnfrsf14* deficiency cooperates with *Bcl2* over-expression in lymphomagenesis [29]. Taken together, inactivation of both *CD274 (PD-L1)* and *TNFRSF14* in thyroid MALT lymphoma most likely abolishes their negative regulation to T-helper cells, hence enhances their function, leading to exaggerated T-cell help to support malignant B-cells (Figure 7).

PD1 governs the localization and function of follicular T-helper cells (TFH) in adaptive immune response. During the germinal centre reaction, PD1/PD-L1 interactions between TFH and B-cells modulate B-cell competition and affinity maturation [27]. PD1/PD-L1 interactions between B and T-cells also regulates their peripheral tolerance [30], and disruption of the PD1/PD-L1 axis can cause a range of autoimmune disorders. In this context, it is worth noting that *PD-L1* mutation/deletion is significantly associated with autoimmune Hashimoto's thyroiditis in patients with thyroid MALT lymphoma. Remarkably, autoimmune thyroiditis and appearance of autoantibodies including anti-thyroperoxidase and anti-thyroglobulin are frequently seen in cancer patients treated with checkpoint inhibitors, particularly with anti-PD1 antibody [31,32]. Thus, PD-L1 inactivation in thyroid MALT lymphoma may impair peripheral tolerance, contributing to the autoimmunity commonly associated with these patients.

There is no detectable PD-L1 expression by immunohistochemistry in thyroid MALT lymphoma, irrespective of *CD274* genetic changes. PD-L1 expression is also not detectable by immunohistochemistry in a range of other low grade B-cell lymphomas as well as in reactive B-cells [33,34]. These findings suggest the absence or a low level of PD-L1 expression that is beyond the sensitivity of immunohistochemistry. In view of the high (constitutive) expression of PD1 in TFH, it is plausible that B-cells may have tightly regulated PD-L1 expression, at a low level, to modulate its interaction with TFH and hence coordinate their cellular activities. In keeping with the above speculations, the proportion of activated T-cells (CD4+CD69+/CD4+) within the vicinity of malignant B-cells was significantly higher in thyroid MALT lymphoma with *CD274/TNFRSF14* inactivation changes than those without these abnormalities. Moreover, the level of transformed blasts was also significantly higher in cases with *CD274/TNFRSF14* inactivation changes than those without these abnormalities. Taken together, *CD274/TNFRSF14* inactivation in malignant B-cells likely deregulates their interactions with T-cells, promoting their co-stimulations.

The finding of remarkably variable involvement of *TET2* mutations in MALT lymphoma of different sites (82% in thyroid, but <8% in other sites) is intriguing as the mutation commonly occurs in haematopoietic stem/progenitor cells in individuals with clonal haematopoiesis of indeterminate potential [11,35]. Nonetheless, *TET2* has a plethora of biological activities as it facilitates DNA demethylation and promotes a permissive chromatin state for transcriptional activities. Apart from a global impact on DNA methylation and gene expression profile, *TET2* also has a locus specific effect, such as regulation of the expression of transcriptional factors critical for B-cell maturation during the germinal centre reaction [20]. *TET2* inactivation by mutation may deregulate the expression of transcriptional factors important for B-cell function, and thus potentially cooperate with receptor signalling, including those by the enhanced T-helper cell signals, indirectly triggered by PD-L1/TNFRSF14 inactivation in malignant B-cells.

Differential diagnosis between thyroid MALT lymphoma and follicular lymphoma could be a challenge, particularly when MALT lymphoma shows prominent follicular colonisation. In most cases, their differential diagnosis could be resolved by carefully integrated investigations of histopathology, immunophenotype, and *BCL2* and *BCL6* translocations [36]. If this conventional approach fails, somatic mutation analysis should assist their differential diagnosis, in light of the remarkable differences in the mutation profile between thyroid MALT lymphoma and follicular lymphoma,[37-39], particularly the highly frequent *CD274* and *TET2* mutations in the former. While *TNFRSF14* mutations are frequent in both MALT and follicular lymphomas, thus offering little value in their differential diagnosis.

In conclusion, thyroid MALT lymphoma is characterised by frequent and concurrent genetic inactivation of both *CD274* and *TNFRSF14*. Their inactivation most likely eliminates their inhibitory regulation to T-helper cells, consequently freeing T-cell function, and providing exaggerated T-cell

help to the lymphoma B-cells. The impaired PD1/PD-L1 interaction may also debilitate peripheral tolerance and contribute to the autoimmunity in patients with thyroid MALT lymphoma. The molecular mechanisms entailed by these genetic changes provide a basis for the development of therapeutic strategies for patients with thyroid MALT lymphoma and Hashimoto's thyroiditis.

Acknowledgements: The authors would like to thank Shubha Anand and Yuanxue Huang for their assistance with using TapeStation, Graeme Clark and Ezequiel Martin for their assistance with Illumina sequencing, and Wanfeng Zhao for help on PD-L1 immunohistochemistry.

Author contributions: Experimental design, data collection and analysis: FW, NW, MMT, CZ, YL, FC, RD, SM, WY, HL, MQD; Illumina sequencing analysis and variant calling: ZC; Multiplex immunofluorescent staining and digital imaging analysis: AA, TM, MQD & NC; Histology review: MQD & CZ; Case contribution: NW, JYN, KI, WZ, WL, JO, AC, YB, SSC, MR; Manuscript writing and preparation: MQD, FW, MMT, FC; Research funding, study design and coordination: MQD, NW, JYL. All authors commented on the manuscript and approve its submission for publication. The authors declare no conflict of interest.

Disclosure of Conflicts of Interest: The authors declare no competing financial interests.

REFERENCES:

1. Du MQ. MALT lymphoma: A paradigm of NF- κ B dysregulation. *Semin Cancer Biol.* 2016;39:49-60.
2. Isaacson PG, Androulakis-Papachristou A, Diss TC, Pan L, Wright DH. Follicular colonization in thyroid lymphoma. *Am J Pathol.* 1992;141:43-52.
3. Hussell T, Isaacson PG, Spencer J. Proliferation and differentiation of tumour cells from B-cell lymphoma of mucosa-associated lymphoid tissue in vitro. *J Pathol.* 1993;169:221-227.

- 408 4. Noy A, de Vos S, Thieblemont C, Martin P, Flowers CR, Morschhauser F *et al.* Targeting Bruton
409 tyrosine kinase with ibrutinib in relapsed/refractory marginal zone lymphoma. *Blood*.
410 2017;129:2224-2232.
- 411 5. Moody S, Escudero-Ibarz L, Wang M, Clipson A, Ochoa Ruiz E, Dunn-Walters D *et al.* Significant
412 association between TNFAIP3 inactivation and biased immunoglobulin heavy chain variable
413 region 4-34 usage in mucosa-associated lymphoid tissue lymphoma. *J Pathol*. 2017;243:3-8.
- 414 6. Hussell T, Isaacson PG, Crabtree JE, Spencer J. The response of cells from low-grade B-cell
415 gastric lymphomas of mucosa-associated lymphoid tissue to *Helicobacter pylori*. *Lancet*.
416 1993;342:571-574.
- 417 7. Greiner A, Knörr C, Qin Y, Sebald W, Schimpl A, Banchereau J *et al.* Low-grade B cell lymphomas
418 of mucosa-associated lymphoid tissue (MALT-type) require CD40-mediated signaling and Th2-
419 type cytokines for in vitro growth and differentiation. *Am J Pathol*. 1997;150:1583-1593.
- 420 8. D'Elia MM, Amedei A, Manghetti M, Costa F, Baldari CT, Quazi AS *et al.* Impaired T-cell
421 regulation of B-cell growth in *Helicobacter pylori*--related gastric low-grade MALT lymphoma.
422 *Gastroenterology*. 1999;117:1105-1112.
- 423 9. Craig VJ, Cogliatti SB, Arnold I, Gerke C, Balandat JE, Wündisch T *et al.* B-cell receptor signaling
424 and CD40 ligand-independent T cell help cooperate in *Helicobacter*-induced MALT
425 lymphomagenesis. *Leukemia*. 2010;24:1186-1196.
- 426 10. Hömig-Hölzel C, Hojer C, Rastelli J, Casola S, Strobl LJ, Müller W *et al.* Constitutive CD40
427 signaling in B cells selectively activates the noncanonical NF-kappaB pathway and promotes
428 lymphomagenesis. *J Exp Med*. 2008;205:1317-1329.
- 429 11. Moody S, Thompson JS, Chuang SS, Liu H, Raderer M, Vassiliou G *et al.* Novel GPR34 and CCR6
430 mutation and distinct genetic profiles in MALT lymphomas of different sites. *Haematologica*.
431 2018;103:1329-1336.

- 432 12. Jung H, Yoo HY, Lee SH, Shin S, Kim SC, Lee S *et al.* The mutational landscape of ocular marginal
433 zone lymphoma identifies frequent alterations in TNFAIP3 followed by mutations in TBL1XR1
434 and CREBBP. *Oncotarget*. 2017;8:17038-17049.
- 435 13. Watanabe N, Narimatsu H, Noh JY, Iwaku K, Kunii Y, Suzuki N *et al.* Long-Term Outcomes of 107
436 Cases of Primary Thyroid Mucosa-Associated Lymphoid Tissue Lymphoma at a Single Medical
437 Institution in Japan. *J Clin Endocrinol Metab*. 2018;103:732-739.
- 438 14. Cucco F, Clipson A, Kennedy H, Sneath Thompson J, Wang M, Barrans S *et al.* Mutation
439 screening using formalin-fixed paraffin-embedded tissues: a stratified approach according to
440 DNA quality. *Lab Invest*. 2018;98:1084-1092.
- 441 15. Clipson A, Wang M, de Leval L, Ashton-Key M, Wotherspoon A, Vassiliou G *et al.* KLF2 mutation
442 is the most frequent somatic change in splenic marginal zone lymphoma and identifies a subset
443 with distinct genotype. *Leukemia*. 2015;29:1177-1185.
- 444 16. Goatly A, Bacon CM, Nakamura S, Ye H, Kim I, Brown PJ *et al.* FOXP1 abnormalities in lymphoma:
445 translocation breakpoint mapping reveals insights into deregulated transcriptional control. *Mod*
446 *Pathol*. 2008;21:902-911.
- 447 17. Yao WQ, Wu F, Zhang W, Chuang SS, Thompson JS, Chen Z *et al.* Angioimmunoblastic T-cell
448 lymphoma contains multiple clonal T-cell populations derived from a common TET2 mutant
449 progenitor cell. *J Pathol*. 2020;250:346-357.
- 450 18. Hu L, Li Z, Cheng J, Rao Q, Gong W, Liu M *et al.* Crystal structure of TET2-DNA complex: insight
451 into TET-mediated 5mC oxidation. *Cell*. 2013;155:1545-1555.
- 452 19. Rajagopal S, Shenoy SK. GPCR desensitization: Acute and prolonged phases. *Cell Signal*.
453 2018;41:9-16.
- 454 20. Schoeler K, Aufschneider A, Messner S, Derudder E, Herzog S, Villunger A *et al.* TET enzymes
455 control antibody production and shape the mutational landscape in germinal centre B cells.
456 *Febs j*. 2019;286:3566-3581.

- 457 21. Supek F, Lehner B, Hajkova P, Warnecke T. Hydroxymethylated cytosines are associated with
458 elevated C to G transversion rates. *PLoS Genet.* 2014;10:e1004585.
- 459 22. Ju X, Zhang H, Zhou Z, Wang Q. Regulation of PD-L1 expression in cancer and clinical
460 implications in immunotherapy. *Am J Cancer Res.* 2020;10:1-11.
- 461 23. Wang Y, Wenzl K, Manske MK, Asmann YW, Sarangi V, Greipp PT *et al.* Amplification of 9p24.1
462 in diffuse large B-cell lymphoma identifies a unique subset of cases that resemble primary
463 mediastinal large B-cell lymphoma. *Blood Cancer J.* 2019;9:73.
- 464 24. Alame M, Pirel M, Costes-Martineau V, Bauchet L, Fabbro M, Tournieret A *et al.* Characterisation
465 of tumour microenvironment and immune checkpoints in primary central nervous system
466 diffuse large B cell lymphomas. *Virchows Arch.* 2020;476:891-902.
- 467 25. Twa DD, Chan FC, Ben-Neriah S, Woolcock BW, Mottok A, Tan KL *et al.* Genomic
468 rearrangements involving programmed death ligands are recurrent in primary mediastinal large
469 B-cell lymphoma. *Blood.* 2014;123:2062-2065.
- 470 26. Green MR, Monti S, Rodig SJ, Juszczynski P, Currie T, O'Donnell E *et al.* Integrative analysis
471 reveals selective 9p24.1 amplification, increased PD-1 ligand expression, and further induction
472 via JAK2 in nodular sclerosing Hodgkin lymphoma and primary mediastinal large B-cell
473 lymphoma. *Blood.* 2010;116:3268-3277.
- 474 27. Shi J, Hou S, Fang Q, Liu X, Liu X, Qi H. PD-1 Controls Follicular T Helper Cell Positioning and
475 Function. *Immunity.* 2018;49:264-274.e264.
- 476 28. Sage PT, Schildberg FA, Sobel RA, Kuchroo VK, Freeman GJ, Sharpe AH. Dendritic Cell PD-L1
477 Limits Autoimmunity and Follicular T Cell Differentiation and Function. *J Immunol.*
478 2018;200:2592-2602.
- 479 29. Mintz MA, Felce JH, Chou MY, Mayya V, Xu Y, Shui JW *et al.* The HVEM-BTLA Axis Restrains T
480 Cell Help to Germinal Center B Cells and Functions as a Cell-Extrinsic Suppressor in
481 Lymphomagenesis. *Immunity.* 2019;51:310-323.e317.
- 482 30. Yao S, Chen L. PD-1 as an immune modulatory receptor. *Cancer J.* 2014;20:262-264.

31. Chalan P, Di Dalmazi G, Pani F, De Remigis A, Corsello A, Caturegli P. Thyroid dysfunctions secondary to cancer immunotherapy. *J Endocrinol Invest.* 2018;41:625-638.
32. de Moel EC, Rozeman EA, Kapiteijn EH, Verdegaal EME, Grummels A, Bakker JA *et al.* Autoantibody Development under Treatment with Immune-Checkpoint Inhibitors. *Cancer Immunol Res.* 2019;7:6-11.
33. Panjwani PK, Charu V, DeLisser M, Molina-Kirsch H, Natkunam Y, Zhao S. Programmed death-1 ligands PD-L1 and PD-L2 show distinctive and restricted patterns of expression in lymphoma subtypes. *Hum Pathol.* 2018;71:91-99.
34. Menter T, Bodmer-Haecki A, Dirnhofer S, Tzankov A. Evaluation of the diagnostic and prognostic value of PDL1 expression in Hodgkin and B-cell lymphomas. *Hum Pathol.* 2016;54:17-24.
35. Cascione L, Rinaldi A, Bruscaggin A, Tarantelli C, Arribas AJ, Kwee I *et al.* Novel insights into the genetics and epigenetics of MALT lymphoma unveiled by next generation sequencing analyses. *Haematologica.* 2019;104:e558-e561.
36. Bacon CM, Diss TC, Ye H, Liu H, Goatly A, Hamoudi R *et al.* Follicular lymphoma of the thyroid gland. *Am J Surg Pathol.* 2009;33:22-34.
37. Nann D, Ramis-Zaldivar JE, Müller I, Gonzalez-Farre B, Schmidt J, Egan C *et al.* Follicular lymphoma t(14;18)-negative is genetically a heterogeneous disease. *Blood Adv.* 2020;4:5652-5665.
38. Pasqualucci L, Khiabanian H, Fangazio M, Vasishtha M, Messina M, Holmes AB *et al.* Genetics of follicular lymphoma transformation. *Cell Rep.* 2014;6:130-140.
39. Cucco F, Barrans S, Sha C, Clipson A, Crouch S, Dobson R *et al.* Distinct genetic changes reveal evolutionary history and heterogeneous molecular grade of DLBCL with MYC/BCL2 double-hit. *Leukemia.* 2020;34:1329-1341.

508 **FIGURE LEGENDS**

509 **Figure 1.** Genetic profile of thyroid MALT lymphoma. Data shown here include chromosome
510 translocations associated with MALT lymphoma, and genes mutated at a frequency of $\geq 3\%$. *CD274*
511 mutation/deletion, *TNFRSF14* and *TET2* mutation are most frequent, often occurring together. For
512 complete genetic data from this study, please see Supplementary Figure S4. CNV: copy number
513 variation.

514

515 **Figure 2.** Distribution and characteristics of *CD274*, *TNFRSF14*, *TET2*, *TNFAIP3*, *CXCR5*, *CXCR3* and
516 *CCR6* mutations in thyroid MALT lymphoma. Where possible, DNA from microdissected non-
517 neoplastic cells was used for PCR and Sanger sequencing to exclude potential germline variants, and
518 mutations confirmed to be somatic are indicated by symbols in red colour.

519 **Figure 3.** Comparison of *CD274*, *TNFRSF14*, *TET2* and *TNFAIP3* mutation AAF (alternative allele
520 frequency) in thyroid MALT lymphoma. Both *TET2* and *TNFRSF14* have a significantly higher
521 mutation AAF than *TNFAIP3*. *TNFRSF14* also has a higher mutation AAF than *CD274*, although not
522 statistically significant.

523 **Figure 4.** Comparison of mutation burden and characteristics according to *TET2* mutation status in
524 thyroid MALT lymphoma. *TET2* mutation is excluded from the mutation calculation. The overall
525 mutation load is significantly higher in the cases with *TET2* mutation than those without the
526 mutation ($P=0.03$). The proportion of transition mutations is also higher in cases with *TET2*
527 mutation than those without the mutation, although not statistically significant.

528 **Figure 5.** Multiplex immunofluorescent staining reveals increased activated T-cells in the vicinity of
529 malignant B-cells harbouring *CD274*/*TNFRSF14* genetic changes.

530

A) An example of multiplex immunofluorescent staining in a case of thyroid MALT lymphoma with both *CD274* and *TNFRSF14* genetic changes; Diffuse tumour areas are marked, and analysed using Halo V3.1 HighPlex FL and proximity modules. GC: germinal centre.

B) Quantitative analysis CD4+/CD20+ cell ratio (left panel), and various CD4+ immunophenotypic subsets within 10µm of CD20+ B-cells. The proportion of activated T cells (CD4+CD69+/CD4+) is significantly higher in cases with *CD274/TNFRSF14* genetic abnormalities than those without these changes.

Figure 6. Correlation between *CD274/TNFRSF14* genetic changes and histological features.

A) Examples of grading for semi-quantification of transformed blasts in thyroid MALT lymphoma; HPF: high power field.

B) Comparison of the extent of transformed blast, plasmacytic differentiation and follicular colonisation between cases with and without *CD274/TNFRSF14* genetic changes. The extent of these histological features was scored as described in the method and compared using the Wilcoxon rank sum test.

Figure 7. Working model of molecular mechanisms underlying thyroid MALT lymphoma.

Inactivation of both *CD274* (PD-L1) and *TNFRSF14* in the lymphoma B-cells abolish their inhibitory regulation to T-helper cells, thus liberating T-cell function, leading to exaggerated T-cell help signals to the lymphoma B-cells.

SUPPLEMENTARY METHODS

SUPPLEMENTARY FIGURES

Supplementary Figure S1. Performance data of 93-gene panel sequencing in thyroid MALT lymphoma. Average depth read and sequence coverage with reads >50 are shown. DNA quality was assessed by a standardised quality control PCR, and 29 samples with suboptimal coverage and/or variants of uncertain (potential false positive) were investigated by the panel sequencing twice.

Supplementary Figure S2. Examples of mutations identified by HaloPlex target enrichment and Illumina Hiseq sequencing in thyroid MALT lymphoma. Aligned reads were transformed to a bam file and visualised using IGV software.

Supplementary Figure S3. Confirmation of *CD274* and *TNFRSF14* somatic mutations in thyroid MALT lymphoma by Sanger sequencing of paired tumour and non-tumour DNA.

Supplementary Figure S4. Mutation profile in various lymphoma entities investigated by 93 gene panel sequencing. Other comprises MALT lymphoma of the lung (n=2) and soft tissue (n=1).
TH_MALT: thyroid MALT lymphoma; OA_MALT: ocular adnexal MALT lymphoma; SA_MALT: salivary gland MALT lymphoma; GA_MALT: Gastric MALT lymphoma; FL: follicular lymphoma; SMZL: splenic marginal zone lymphoma; AITL: angioimmunoblastic T-cell lymphoma; MEITL: monomorphic epitheliotropic intestinal T-cell lymphomas.

Supplementary Figure S5. Detection of CD274 deletion in thyroid and salivary gland MALT lymphoma by multiplex ligation-dependent probe amplification (MLPA). A) A schematic illustration of the three genes covered by the MLPA probes. B) Heatmap illustration of the normalised amplification signal. Each column denotes a case (TM: thyroid MALT lymphoma; SM: salivary gland MALT lymphoma).

Supplementary Figure S6. Absence of PD-L1 expression in thyroid MALT lymphoma. A representative case shows negative PD-L1 immunostaining in malignant B-cells and most of intact thyroid epithelial cells, but positive staining in epithelial cells involved in lymphoepithelial lesions.

SUPPLEMENTARY TABLES

Supplementary Table S1: Lymphoma entities and number of cases successfully investigated.

Supplementary Table S2: List of 93-genes investigated by targeted sequencing.

Supplementary Table S3. Primers used for PCR and Sanger sequencing of the *CD274* and *TNFRSF14* genes.

Supplementary Table S4: Antibodies and reagents used for immunofluorescence or immunohistochemical staining

Supplementary Table S5: Variants detected by 93-gene panel sequencing.

Supplementary Table S6. Clinical features and correlations with *CD274/TNFRSF14/TET2* changes and histological features.

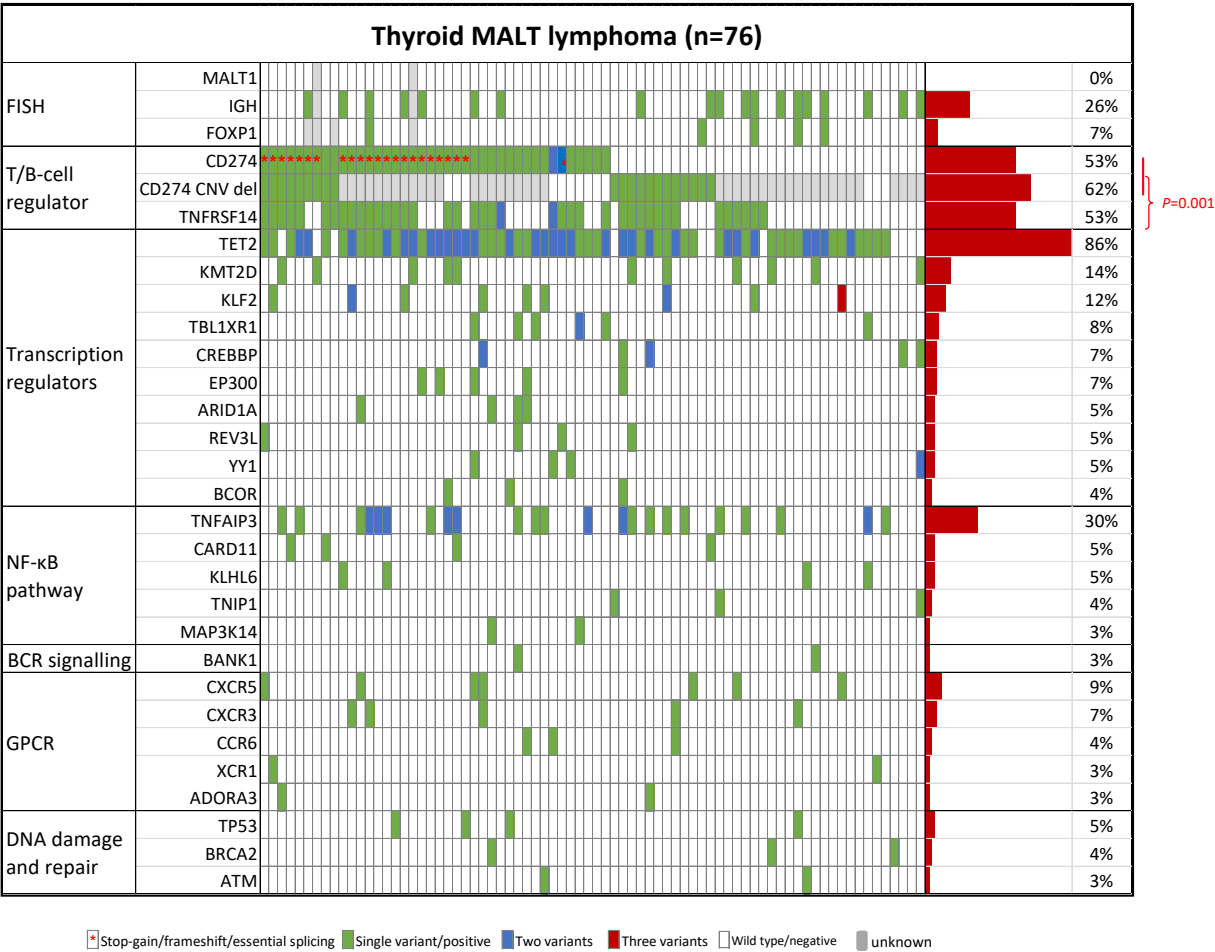


Figure 1. Genetic profile of thyroid MALT lymphoma. Data shown here include chromosome translocations associated with MALT lymphoma, and genes mutated at a frequency of $\geq 3\%$. *CD274* mutation/deletion, *TNFRSF14* and *TET2* mutation are most frequent, often occurring together. For complete genetic data from this study, please see Supplementary Figure S4

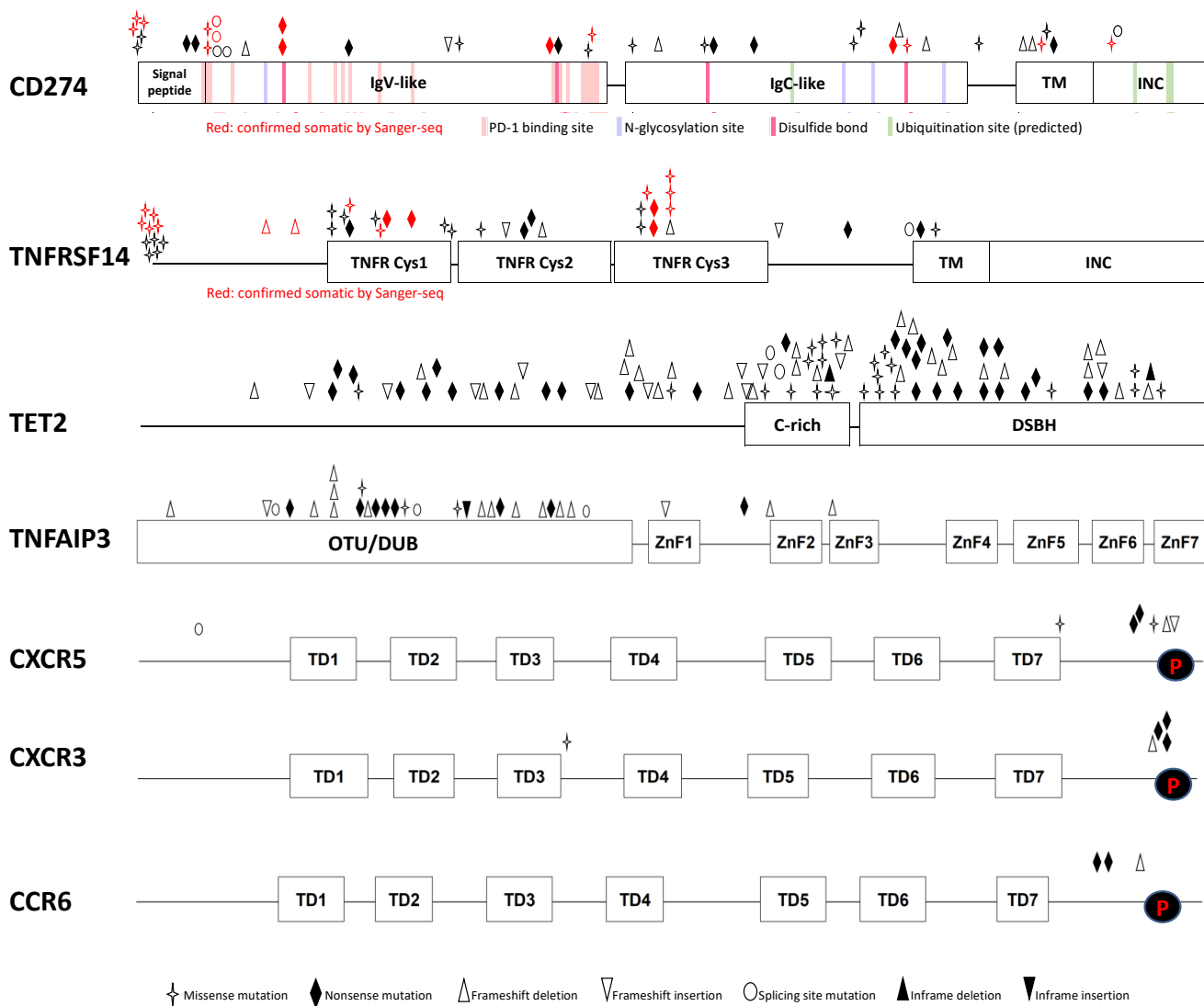


Figure 2. Distribution and characteristics of *CD274*, *TNFRSF14*, *TET2*, *TNFAIP3*, *CXCR5*, *CXCR3* and *CCR6* mutations in thyroid MALT lymphoma. Where possible, DNA from microdissected non-neoplastic cells is used for PCR and Sanger sequencing to exclude potential germline variants, and mutations confirmed to be somatic are indicated by symbols in red colour. **P** Predicted phosphorylation site.

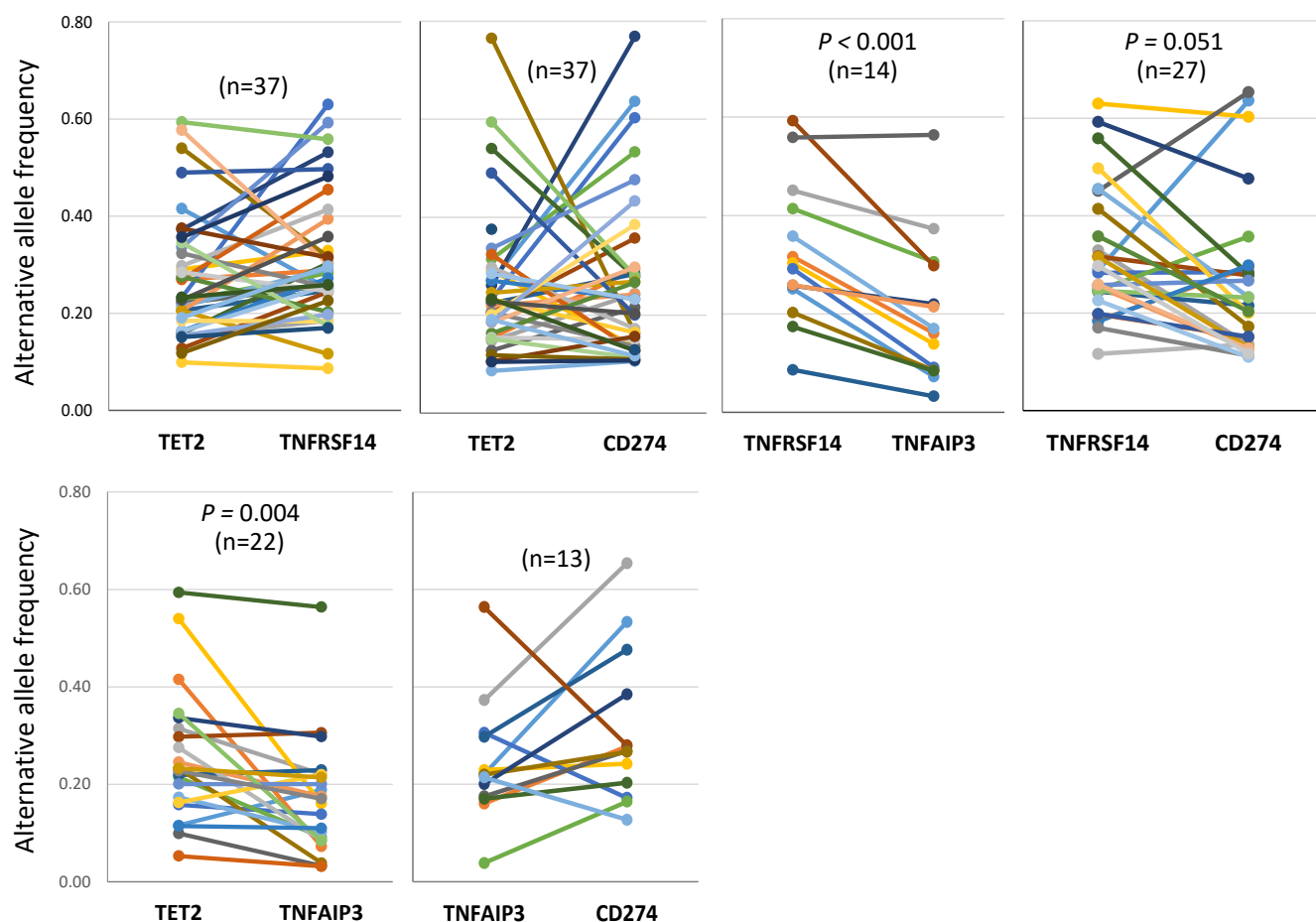


Figure 3. Comparison of *CD274*, *TNFRSF14*, *TET2* and *TNFAIP3* mutation AAF (alternative allele frequency) in thyroid MALT lymphoma. Both *TET2* and *TNFRSF14* have a significantly higher mutation AAF than *TNFAIP3*. *TNFRSF14* also has a higher mutation AAF than *CD274*, but not statistically significant.

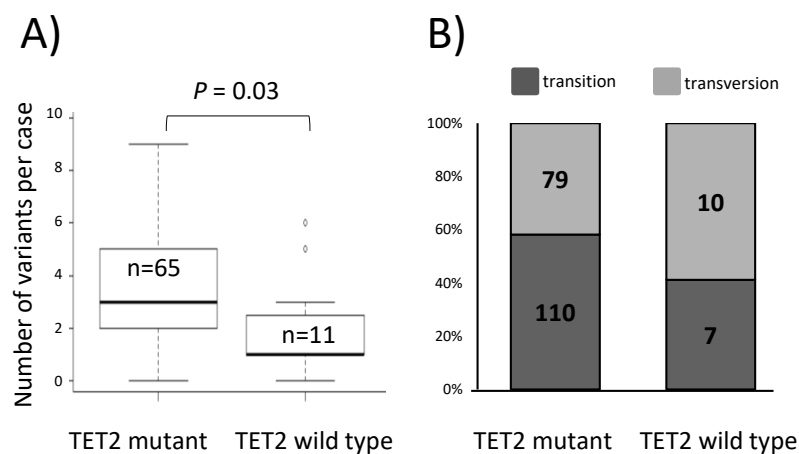


Figure 4. Comparison of mutation burden and characteristics according to *TET2* mutation status in thyroid MALT lymphoma. *TET2* mutation is excluded from the mutation calculation. The number of variants (excluding SNPs) is significantly higher in the cases with *TET2* mutation than those without the mutation ($P=0.03$). The proportion of transition mutations is also higher in cases with *TET2* mutation than those without the mutation, although not statistically significant.

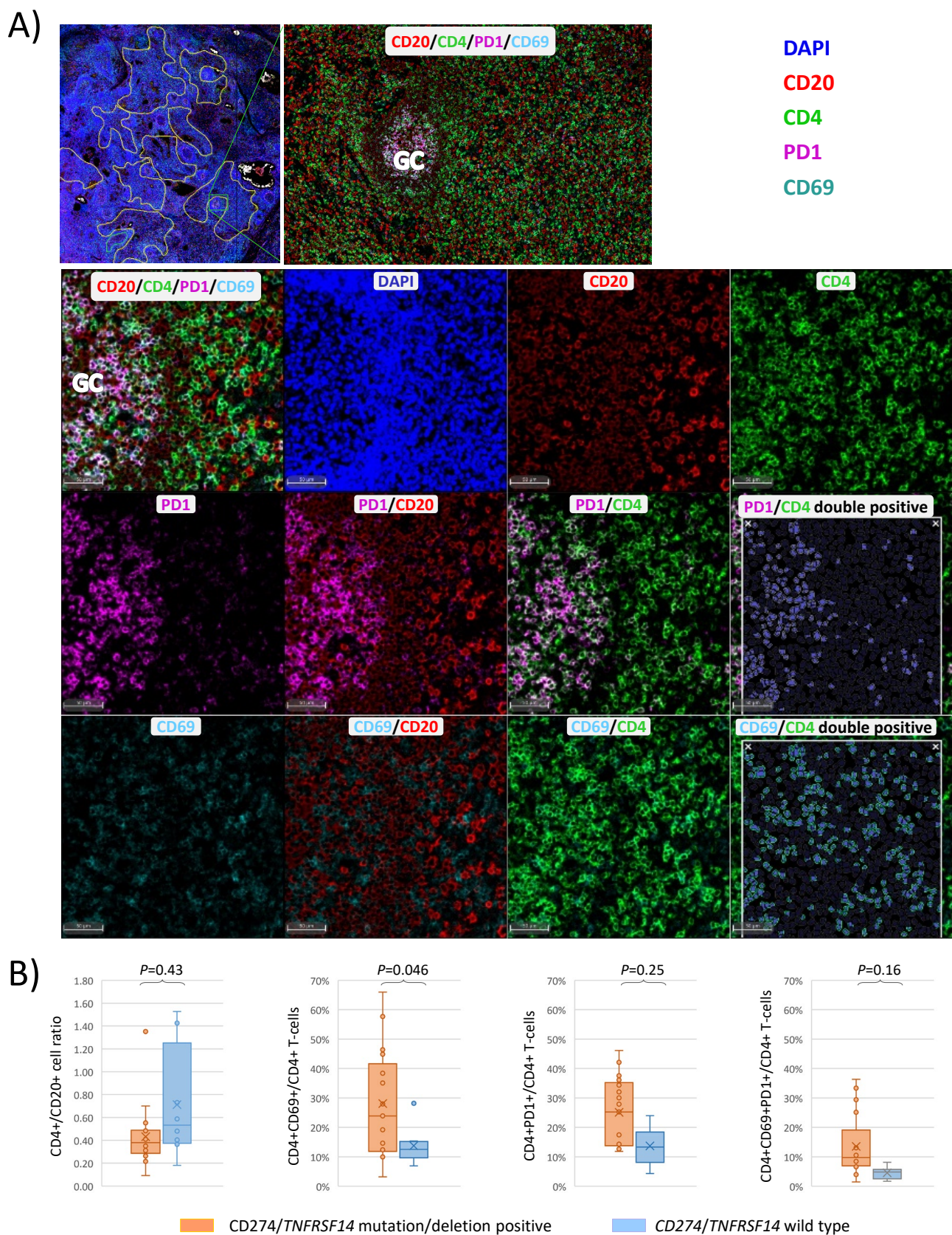


Figure 5. Multiplex immunofluorescent staining reveals increased activated T-cells in the vicinity of malignant B-cells harbouring *CD274/TNFRSF14* genetic changes.

A) An example of multiplex immunofluorescent staining in a case of thyroid MALT lymphoma with both *CD274* and *TNFRSF14* genetic changes; Diffuse tumour areas are marked, and analysed using Halo V3.1 HighPlex FL and proximity module. GC: germinal centre.

B) Quantitative analysis CD4+/CD20+ cell ratio (left panel), and various CD4+ immunophenotypic subsets within 10µm distance of CD20+ B-cells. The proportion of activated T cells (CD4+CD69+/CD4+) is significantly higher in cases with *CD274/TNFRSF14* genetic abnormalities than those without these changes.

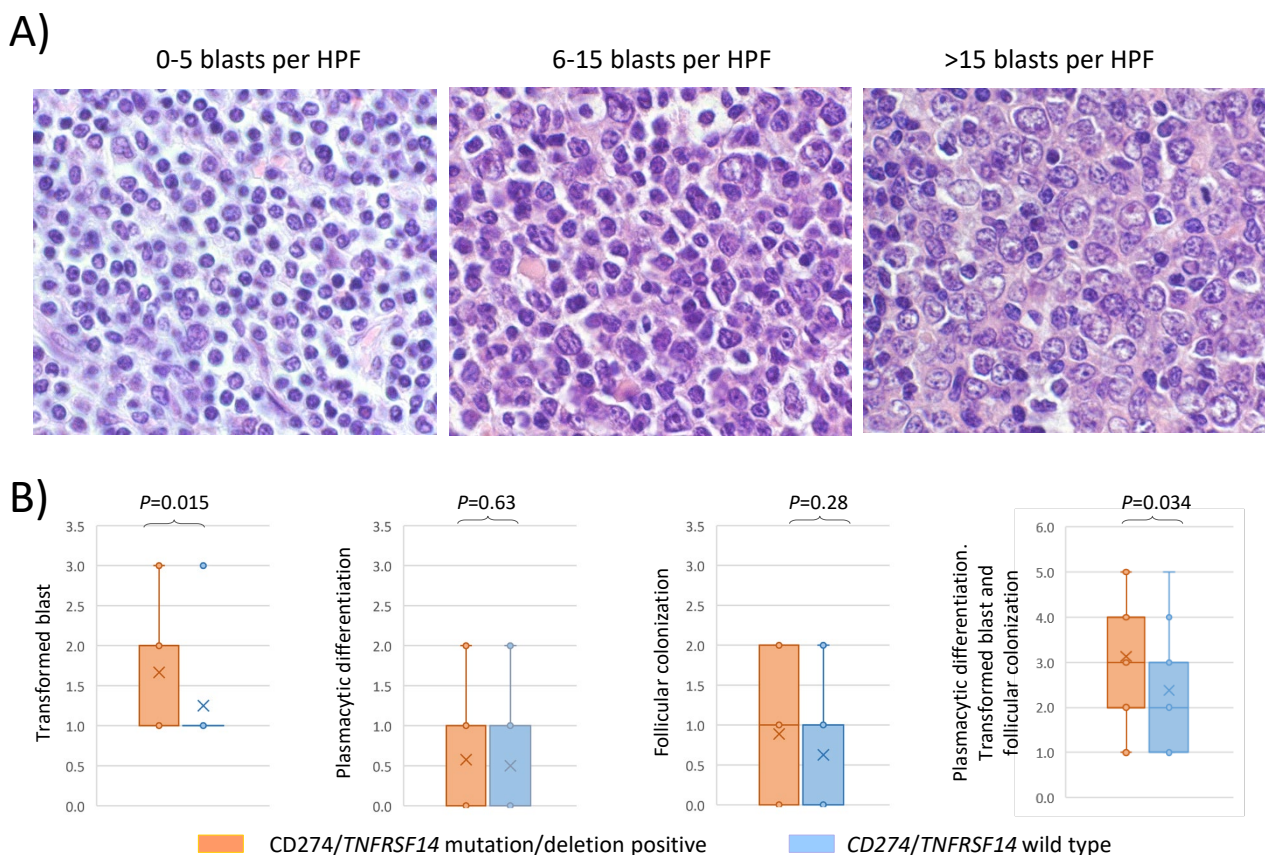


Figure 6. Correlation between *CD274/TNFRSF14* genetic changes and histological features.

- A) Examples of grading for semi-quantification of transformed blasts in thyroid MALT lymphoma;
- B) Comparison of the extent of transformed blast, plasmacytic differentiation and follicular colonisation between cases with and without *CD274/TNFRSF14* genetic changes. The extent of these histological features was scored as described in the method and compared using the Wilcoxon rank sum test.

HPF: high power field.

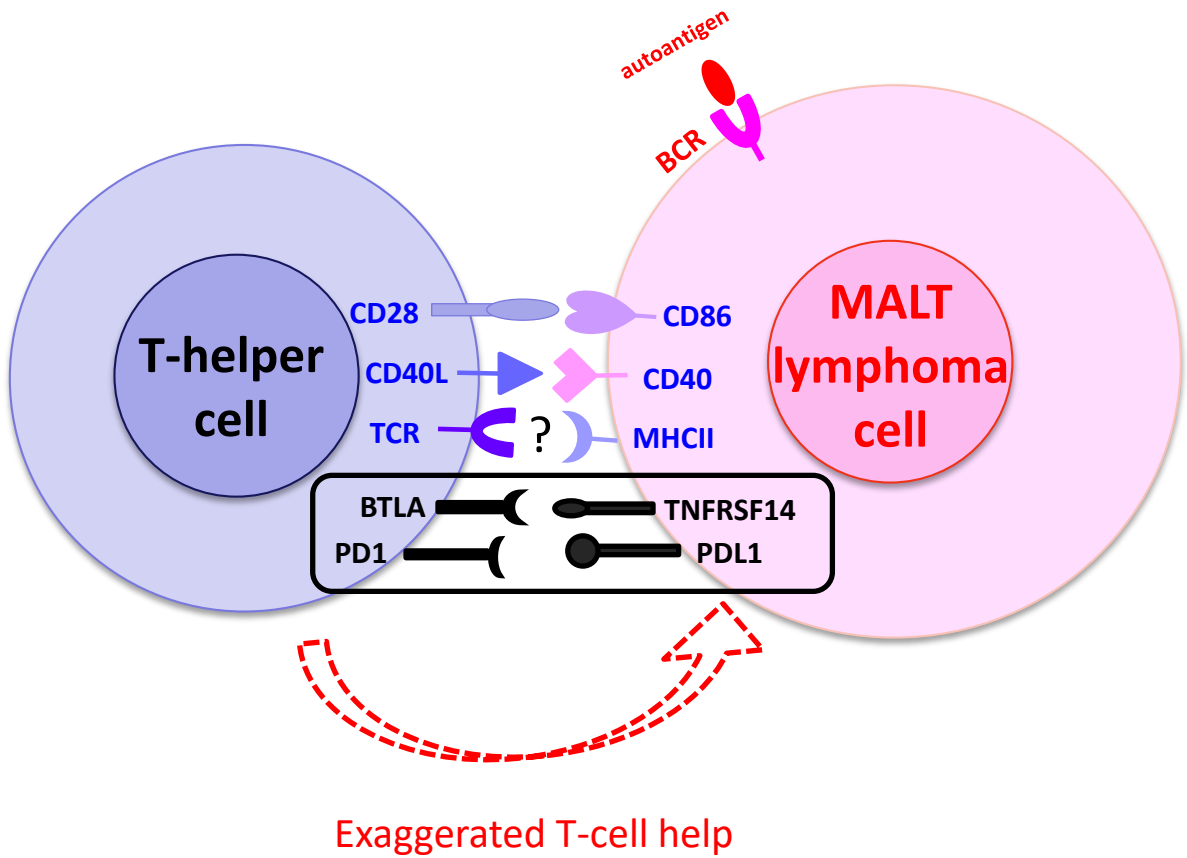


Figure 7. Working model of molecular mechanisms underlying thyroid MALT lymphoma. Inactivation of both *CD274* (PD-L1) and *TNFRSF14* in the lymphoma B-cells abolish their inhibitory regulation to T-helper cells, thus liberating T-cell function, leading to exaggerated T-help signals to the lymphoma B-cells.